

SYNTHESIS OF DENTAL FLUOROAPATITE GLASS-CERAMIC GLAZES

G. ABOLFATHI, #B. EFTEKHARI YEKTA

*Department of Material Science, Ceramic Division,
Iran University of Science and Technology, Tehran, Iran*

#E-mail: beftekhari@iust.ac.ir

Submitted March 15, 2011; accepted September 26, 2011

Keywords: Glass-ceramic glaze, Dental, Fluoroapatite, Lithium disilicate

A dental glass-ceramic glaze based on the $\text{SiO}_2\text{-Li}_2\text{O}_3\text{-P}_2\text{O}_5\text{-CaO}$ system, which is currently used as dentin for lithium-disilicate glass-ceramic cores, was synthesized. The role of Na_2O , CaO and P_2O_5 in sintering and crystallization of the related glasses were studied by firing at temperatures higher than their dilatometric softening point. Sintering of glasses led to precipitation of needle - like fluoroapatite crystalline particles. However, in spite of current definition about glass-ceramics, the final synthesized composition and a similar trade mark sample, which was used as reference, did not show considerable amounts of crystalline phases after sintering process. Furthermore, reducing the constituent 's of fluoroapatite in glass composition led to reduction of sinterability and fusibility of the system.

INTRODUCTION

Glass-ceramics are polycrystalline materials, which are prepared by controlled crystallization of glasses. This controlled crystallization is intended and leads to precipitation of tiny crystalline particles [1,2]. The density, growth rate and the ultimate dimension of crystalline particles are controlled by composition and heat-treatment procedure. Due to their bio-compatibility, most glass-ceramics can be used extensively in medical profession and dentistry, e.g. as dental cores, glazes, etc. (3). A group of these materials named lithium disilicate ($\text{Li}_2\text{Si}_2\text{O}_5$) glass-ceramics are used in dentistry for restoration of anterior and posterior crowns and all-ceramic bridges [3]. Some fluoroapatite ($\text{Ca}_5(\text{PO}_4)_3\text{F}$) - based glass ceramics, like IPS e.max Ceram, have been designed as veneer for use in conjunction with the above-mentioned all ceramic system [4]. The nano-scale fluoroapatite crystals are responsible for the opalescence of these kinds of veneer materials and therefore contribute to its aesthetic properties. In addition, the material's opacity is mainly determined by the larger fluoroapatite crystals. However, in spite of extensive use of these kinds of veneer glazes there is not any scientific published works about these materials. Therefore, synthesizing a glass-ceramic glaze containing

fluoroapatite crystals and investigating the mechanism of its crystallization and flow ability behavior of the glazes during firing and also the roles of minor ingredients on these mentioned specifications seems to be necessary and were the aim of the present work. In this way, the mechanism of crystallization and the sinterability of an adopted optimum glaze and the similar commercial one, i.e. IPS e.max Ceram, were investigated and compared with each other.

EXPERIMENTAL

Table 1 shows the glass compositions, which were used in the present experiment. G1 was the base glass, adopted from the literature [4]; the others were prepared by changing the amounts of fluoroapatite constituents, i.e. CaO and P_2O_5 , as well as Na_2O .

The used raw materials were reagent grades silica, alumina, calcium carbonate, phosphorus pentoxide, potassium nitrate, zinc oxide, sodium carbonate and calcium fluoride powders. The raw materials were thoroughly mixed and then melted in high purity alumina crucibles, in an electric kiln at 1450°C for 2 h. The melts were then quenched in cold distilled water. The resulted frits were wet milled by hard porcelain planetary mill to particle sizes less than $30\ \mu\text{m}$.

Table 1. Chemical composition of glasses (wt. %).

Glass	SiO ₂	Al ₂ O ₃	Na ₂ O	K ₂ O	ZnO	F	P ₂ O ₅	CaO	Li ₂ O
G1	63.7	8.0	7.5	6.0	3.0	0.8	4.0	5.0	2.0
G2	63.7	8.0	7.5	6.0	3.0	0.8	4.0	3.0	2.0
G3	63.7	8.0	7.5	6.0	3.0	0.8	2.0	5.0	2.0
G4	63.7	8.0	5.5	6.0	3.0	0.8	4.0	5.0	2.0

Crystallization temperature and the mechanism of crystallization were investigated by Differential Thermal Analysis (STA; Polymer Laboratories 1640). A similar trade mark sample (IPS e. max Ceram) made by the Ivoclar Vivadent Co. was also examined and compared with the prepared glasses in this regard. The thermal expansion coefficient and the dilatometric softening point of the prepared glass-ceramic glazes were determined by the dilatometric method (Netzsh, E402). The crystalline phases that were precipitated in the fired samples were identified using X-ray diffractometer (Jeol JDX-8030). Microstructures of the samples were evaluated by scanning electron microscope (Cambridge-S360) after polishing (up to 1 μm diamond paste) and etching in 5% HF solution for 15 s. A Vickers micro-hardness tester with a diamond pyramid (MXT-AL, MX 9660a) was used to measure the micro hardness of glaze by applying a load of 50 g for 15 s. Bending strength of samples was evaluated as a glaze layer, according to ISO 6872(2008). The substrate was a commercial dental lithium disilicate - based glass-ceramic named IPS emax press. Ten polished rectangular specimens (25 \times 5 \times 2 mm) were tested for each series of glazes.

The chemical resistance of specimens was determined according to ISO 6872. Accordingly, the solubility of the immersed samples in a hot (80°C) 4% acetic acid solution was considered as a criterion of the chemical resistance for them.

RESULTS AND DISCUSSION

Figures 1a and 1b depict the particle size distribution of the base and the commercial glasses, respectively. As the particle size distribution of glass powder affects considerably the sinterability and crystallization of the compacted bodies, it was tried to keep it constant for all samples. Accordingly, the mean and maximum particle sizes of both powders were about 10 and 25 μm , respectively.

Figure 2 shows the DTA thermographs of G1 and the reference glasses. As no exothermic peak can be detected in the two DTA thermographs, it can be concluded that either surface crystallization should be the dominate mechanism of crystallization or only a negligible crystalline phase precipitates in them during the experiments.

Densification of compacted glass particles occurs through viscous flow mechanism. This mechanism becomes active above the dilatometric softening point of glass. Hence, to find the least temperature of sintering, dilatation behavior of the glasses with temperature was determined (Figure 3). As the dilatometric softening point of G1 was about 550°C, higher temperatures were adopted for simultaneous sintering and crystallization of it and the reference sample. Figures 4a and 4b show the side-views of the two compacted glass powders, after

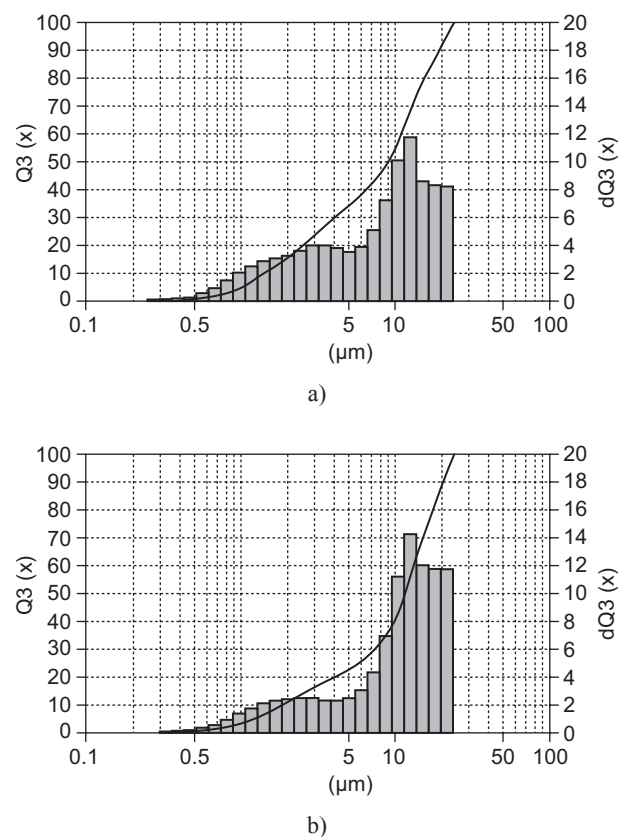


Figure 1. Particle size distribution of the base glass (a) and the commercial glass (b).

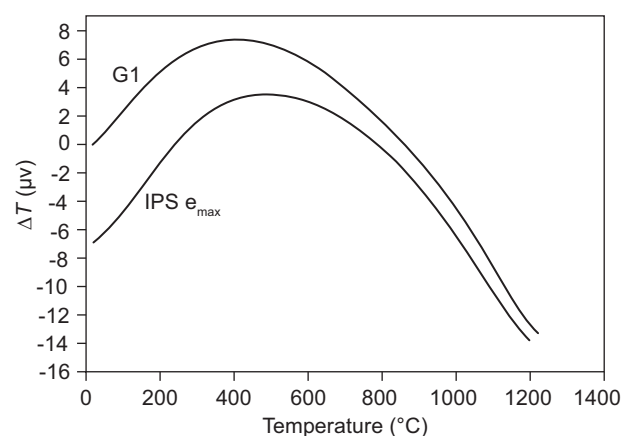


Figure 2. DTA traces of the G1 and the commercial glasses.

sintering at 750 and 820°C, respectively. It can be seen that while the two glasses do not show any considerable densification at 750°C, they show fluidity and a glazy appearance at 820°C.

Figures 5a and 5b show respectively the X-ray diffraction patterns of G1 and the reference sample after sintering at various temperatures for 10 min. Because of the low intensity patterns, especially in the G1, precise identification of the precipitated crystalline phases was extremely difficult. However, it can be said hardly that fluoroapatite, lithium disilicate and perhaps rhenanite (NaCaPO₄) had been crystallized in the glasses during heating. It means that in spite of recommended scientific definition for glass-ceramics, only a negligible crystallization has taken place in the two glasses during sintering. It seems that the extremely low melting temperature of these glasses makes them more stable and so keeps them from an extensive crystallization [5].

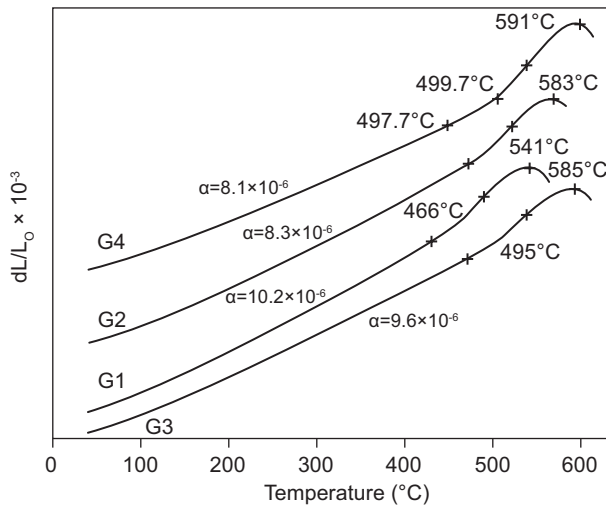


Figure 3. Dilatometry traces of the prepared glasses G1, G2, G3 and G4.

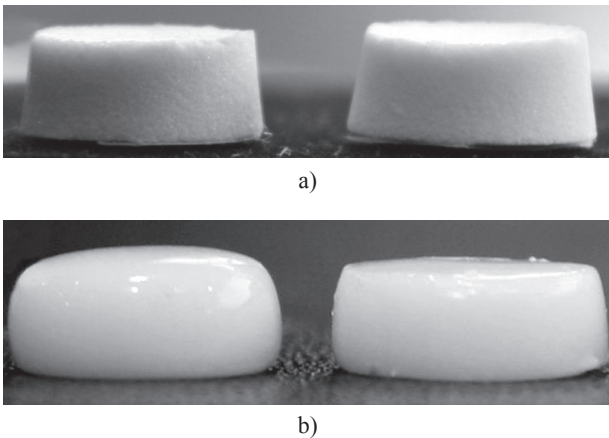
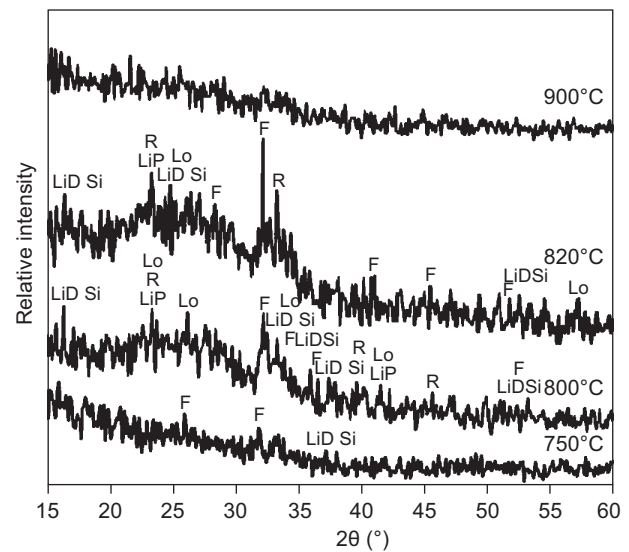


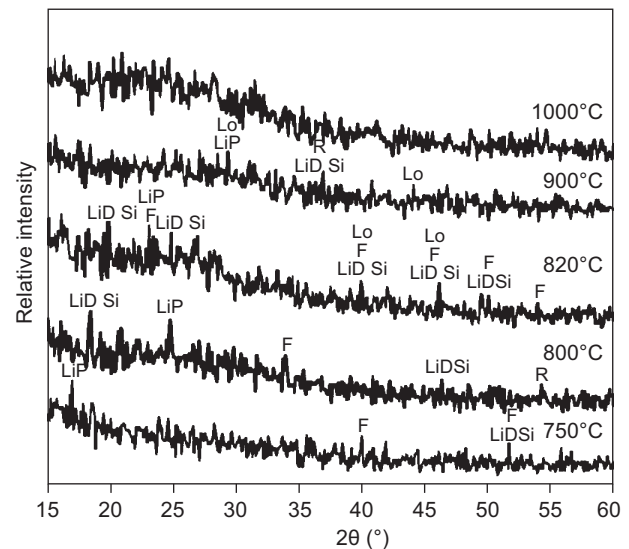
Figure 4. The profiles of compacted glass specimens after firing at a) 750°C and b) 820°C. The left side specimen is the reference glass and the right side one is G1 in each picture.

It should be mentioned that increasing of firing temperature to 900°C led slightly to reduction of X-ray diffraction patterns intensity (see Figures 5a and 5b), possibly due to solubility of crystalline phases in the residual glass phase.

The as-received frit G1 was milky. Its X-ray diffraction patterns showed that it contained a small amount of fluoroapatite. In order to suppress this event that could delay the densification and flow-ability of glass-ceramic specimens [6,7], reducing the amounts of fluoroapatite constituents was considered. It is said that rhenanite acts as a nuclei for precipitation of fluoroapatite [8].



a) reference



b) G1

Figure 5. X-ray diffraction patterns of a) the reference and b) G1, after sintering at different temperatures for 10 min (LiD Si - Li₂Si₂O₅; LiP - Li₃PO₄; F - Ca₅(PO₄)F; Lo - KAlSi₂O₆; R - NaCaPO₄).

Therefore, it was assumed that reducing or omitting of rhenanite, by reduction of its constituents, should also be helpful in this regard. Accordingly, glasses G2, G3 and G4 were prepared (Table 1). The frits of these new glasses were more transparent; however, as CaO, P₂O₅ and Na₂O usually act as flux in the glass composition, these changes in glass composition led to undesirable rising of the softening point (Figure 3) and fusibility temperatures of the new glasses (Figure 6).

X-ray diffraction patterns of the fired G2, G3 and G4 at 820°C and 900°C (for 10 min) indicate that the same crystalline phases have precipitated in them in both temperatures (Figure 7); and contrary to G1, the intensity of their patterns increases with increasing of firing temperature to 900°C. Beside, according to the dilatometric results, the thermal expansion coefficient of the fired glazes G1, G2, G3 and G4 between 25-400°C was 10.2, 8.3, 9.6 and 8.1×10⁻⁶/°C, respectively. Finally, regarding of sintering and crystallization behaviors of the glasses, it can be concluded that G1 was more similar in point of fusibility view to the reference sample.

Figure 8 shows the microstructures of the glass G1 after firing at 820°C, a) without a soaking time and b) with a soaking time of 5 min. It is expected that if surface crystallization begins prior to viscous flowing of

glass at the initial step of sintering procedure, each glass particle in the compacted specimen should be separated by crystallized grain boundaries [9]. However, there is not any sign in the above-mentioned microstructures to show such condition. As it was expected from the low amounts of crystalline phases in the fused G1, it seems that the glass particles have flowed together and formed a monolithic body during the firing procedure and prior to starting of crystallization.

Figures 9a and 9b show the microstructures of the reference and G1 glazes after firing at 820°C for 10 min. In these micrographs mostly the particles which are situated perpendicularly to the surface are observed. Apparently, other particles had been removed a way from the surface during grinding and polishing of specimens and leaved elongated empty spaces on the surface. This situation is more obvious in Figure 9a. The arrows show the needle-like fluoroapatite crystals in both microstructures. It can be seen that G1 contained finer particles. Figure 10 shows also the microstructure of a rapidly cooled glass G1. The X-ray diffraction pattern of this sample showed that it was completely amorphous. Accordingly, it seems that the glass has experienced a nucleation type mechanism of liquid- liquid phase separation during cooling to room temperature. In compositions similar to that of glass G1 elements like P, F, and Ca concentrate within the



Figure 6. The profiles of compacted glasses after firing at 820°C for 10 min, from left to right, the reference, G1, G2, G3 and G4 glasses, respectively.

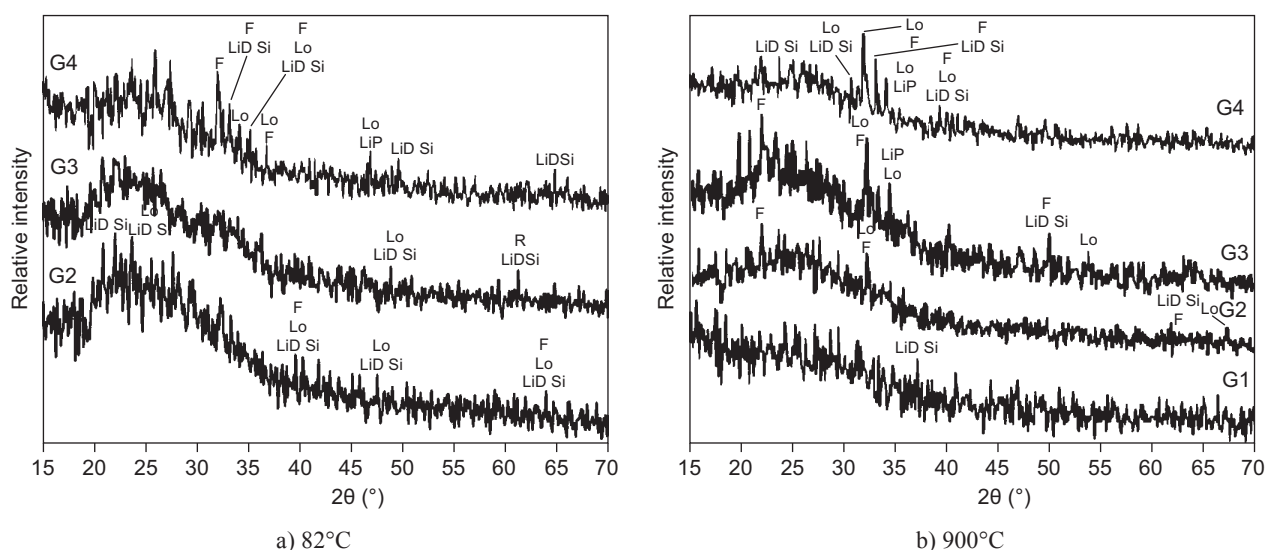


Figure 7. X-ray diffraction patterns of G2, G3 and G4, after firing at a) 820°C and b) 900°C for 10 min. (LiD Si - Li₂Si₂O₅; LiP - Li₃PO₄; F - Ca₅(PO₄)F; Lo - KAlSi₂O₆; R - NaCaPO₄).

droplets during separation [9, 10] and make these areas susceptible for precipitation of needle-like crystals of fluoroapatite during post-firing. Comparing the Figures 9b and 10, it seems that a similar event has taken place in the G1.

The two fired glazes showed also different behavior when they applied on lithium disilicate-based glass-ceramic substrate, named IPS emax press. Figures 11 and 12 depict the interfaces of substrate-glaze layers of the two samples after firing at 820°C for 10 min. Based on these figures, while a thick interface layer has formed between the lithium disilicate-based glass-ceramic

substrate and glaze G1, there is a thin and sharp interface between the substrate-reference glaze layers. This discrepancy can be initiated from different reactivity of the two glazes; accordingly, G1 is more reactive than the reference glaze. Figure 13 shows the line scan analysis of substrate-interface-glaze layers of G1 specimen, based on the Ca, Al and Si elements. According to these analyses, while the lithium disilicate-based glass-ceramic substrate has a higher Si, which decreased gradually in the interface layer, the amounts of Ca and Al elements are higher in the glaze composition than the substrate. This change in the intermediate layer indicates a higher

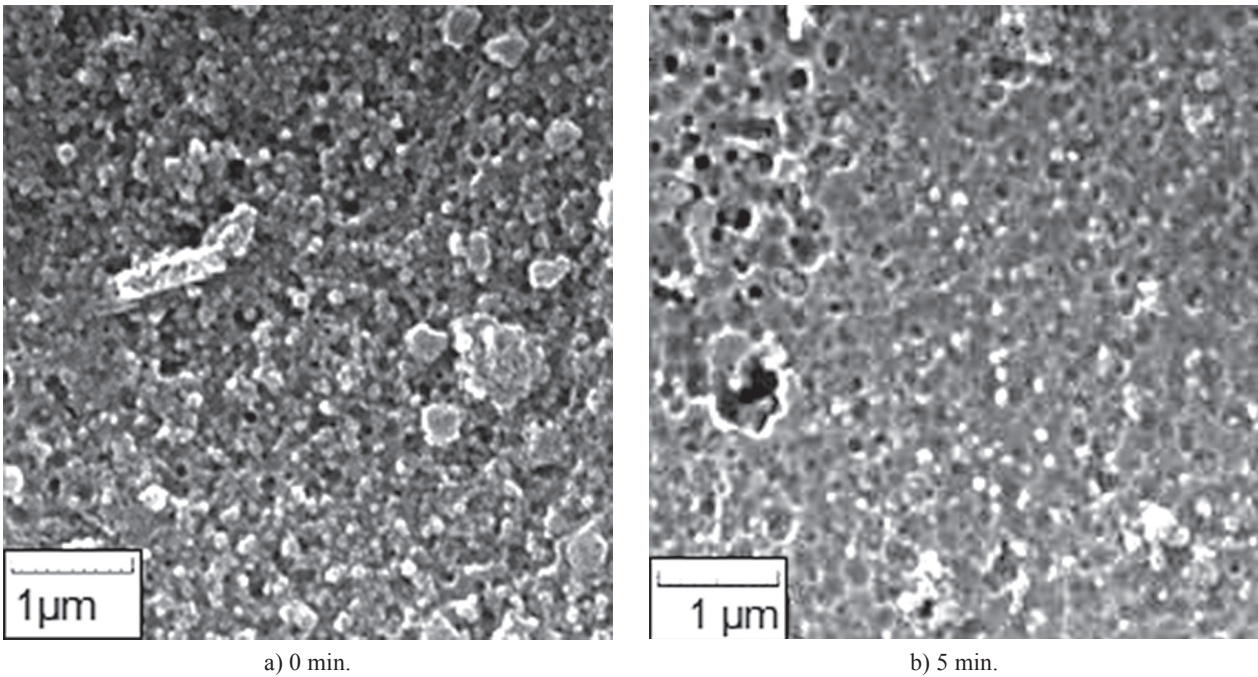


Figure 8. Microstructures of Glass G1 after firing at 820°C with a soaking of a) 0 and b) 5 min.

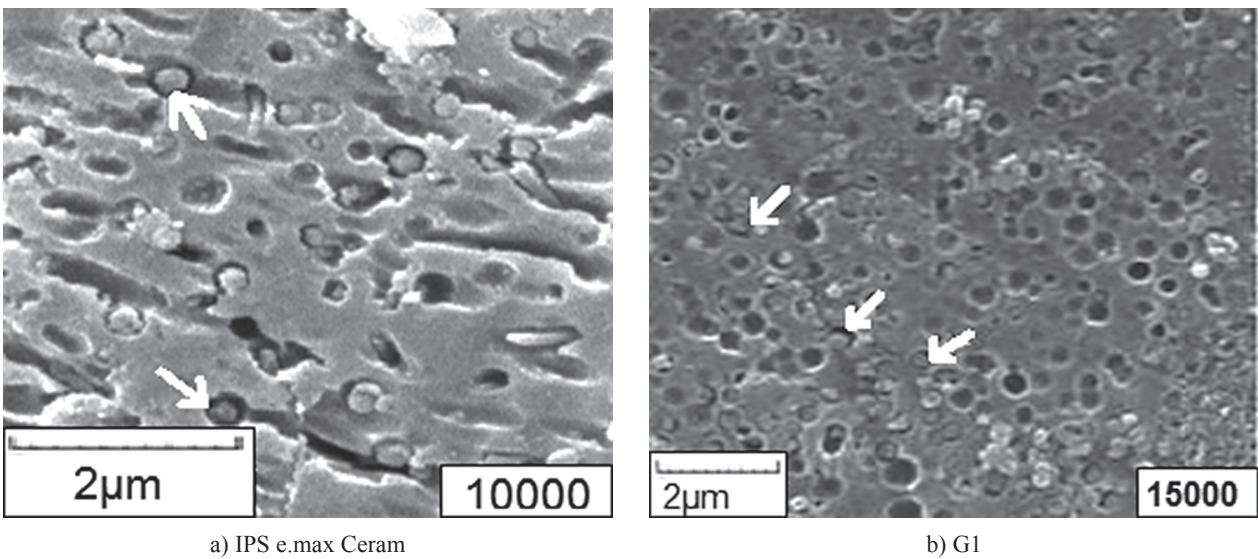


Figure 9. Microstructures of glazes a) IPS e.max Ceram and b) G1, after firing at 820°C for 10 min.

solubility of substrate in the glaze layer G1 and reduces the ability of crystallization for glaze in this region.

Table 2 shows the Vickers micro-hardness, bending strength and the chemical resistance of glasses G1 and the reference. The micro-hardness of glasses was determined in two different states, as a thin glaze layer and as a bulk vitreous body. As it can be seen, while the two bulk vitreous samples show nearly the same micro-hardness, G1 shows higher hardness when it was used as a glaze layer. However, the substrate glazed by G1 shows a lower bending strength than the other. These contradictory results probably originate from statistically nature of mechanical properties of ceramics and it is

difficult to involve the effect of thermal expansion coefficients of substrate- glazes in the mentioned observations. It is also can be seen that G1 has a less solubility than the reference sample which is indicative of its higher chemical resistance, probably due to its lower alkaline oxides.

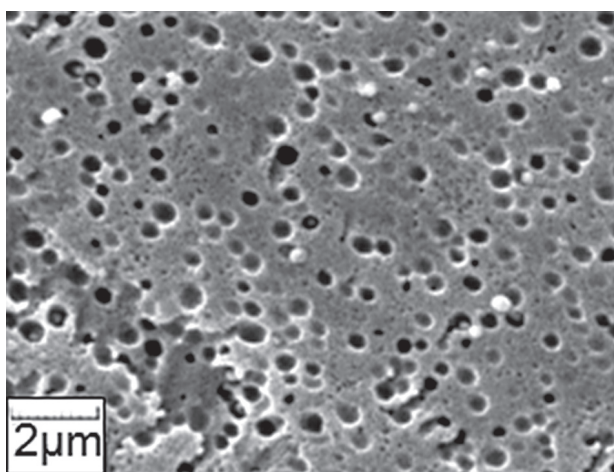


Figure 10. Microstructure of a rapidly cooled as-received glass G1, after etching by a 5% HF acid for 15 s.

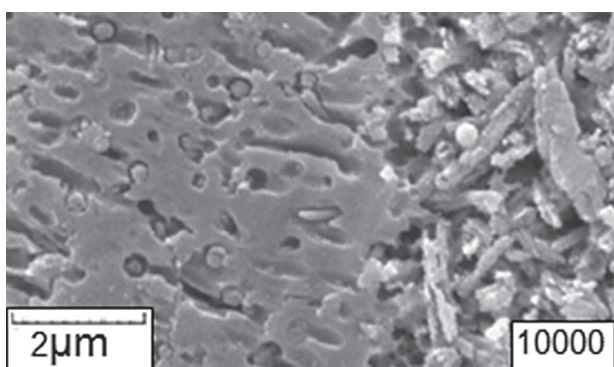


Figure 11. The substrate - reference glaze interface.

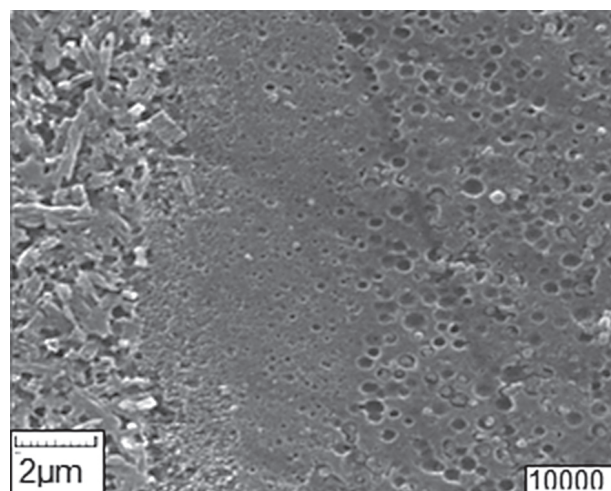


Figure 12. The substrate - G1 glaze interface.

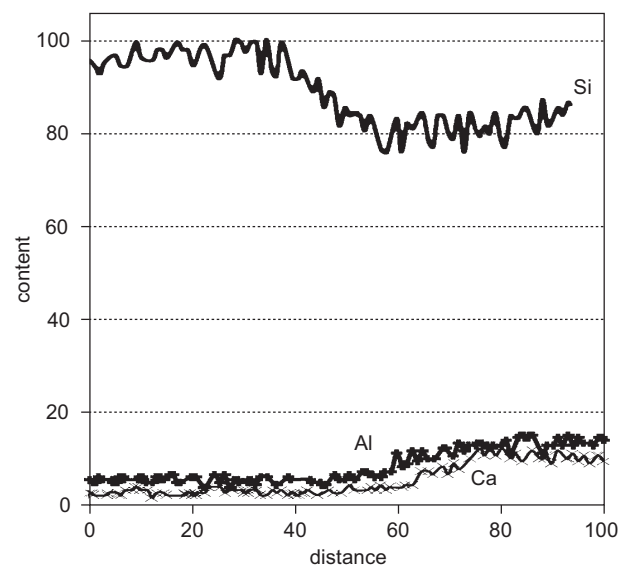


Figure 13. Line scan analysis of substrate - G1 glaze interface based on Ca, Al and Si elements.

Table 2. Vickers micro-hardness, bending strength and chemical solubility of G1 and the reference sample.

Property	G1		Reference sample	
	Bulk vitreous body	Glaze layer	Bulk vitreous body	Glaze layer
Vickers micro-hardness	283 ± 57	333 ± 105	294 ± 153	253 ± 123
Thermal expansion 25-400°C × 10 ⁻⁶ (1/K)		10.2		9.5
Bending strength of the glazed substrate (MPa)		239.45		258.0
Chemical solubility(μg/cm ²)		11.65		42.16

CONCLUSIONS

Regardless of recommended definitions about glass-ceramics, the amounts of precipitated crystalline phases in both the fired reference glaze and G1 were considerably low. It seems that demand for a low firing temperature obligates a low precipitation of crystalline phases in this kind of compositions.

A nucleation mechanism of liquid - liquid phase separation took place within the optimum glass composition (G1) prior to crystallization of needle-like fluoroapatite crystals and during cooling of the glass melt. The thermal expansion coefficient and chemical solubility of the optimum glaze specimen (G1) were respectively $10.2 \times 10^{-6} 1/^{\circ}\text{C}$ between the 25-400°C, and $11.65 \mu\text{g}/\text{cm}^2$, which indicate G1 is suitable for veneering of lithium disilicate based glass-ceramic cores.

References

1. Escardino Benlloch A.: *Cer. Acta* 8, 5 (1996).
2. Kingery W.D., Bowen H.K., Uhlmann D.R.: *Introduction to Ceramics*, Second Edition, pp. 368-375, John Willey & Sons, New York 1975.
3. Holand W., Beall G.: *Glass-ceramic technology*, pp.272-309, American Ceramic Society, Westerville, 2002.
4. Ivoclar Vivadent, Scientific Documentation IPS e.max® Ceram, page 6.
5. Rawson H. in: *Proc. 4th Inter. Congr. on glass*, Imprimerie Chaix, Paris, 1956.
6. Eftekhari Yekta B., Marghussian V.K.: *J. Mat. Sci.* 36, 477 (2002).
7. Knickerbocker S.H., Kumar A.H., Herron C.W.: *Am. Ceram. Soc. Bull.* 72, 91 (1993).
8. Aple E., Hoen C., Rheinberger V., Holand W.: *J. Eur. Ceram. Soc.* 27, 1571 (2007).
9. Zheng X., Wen G., Song L., Houang X.X.: *Acta Materialia* 56, 549 (2008).
10. Wen G., Zheng X., Song L.: *Acta Materialia* 55, 3583 (2007).